Temperature investigation in contact pantograph - AC contact line

Constantin-Florin OCOLEANU, Ioan POPA, Gheorghe MANOLEA, Alin-Iulian DOLAN, Serghie VLASE

Abstract— In this paper we performed a thermal analyses using experimental determination of temperature in contact pantograph - AC contact line. The pantograph is asymmetric EPC type and the contact line wire is TF 100 type, both used in Romanian Electric Railways. The influence on the temperature value of the small contact area between two collector strips of pantograph and contact wire is pointed out..

Keywords— asperity, contact area, contact resistance, contact wire line, electric railway, pantograph.

I. Introduction

The contact between pantograph and AC electric railway system supply contact line is studied in literature and represents an important problem concerning the exploitation of rails vehicles. The pantograph - catenary system is still today the most reliable form of collecting electric energy for the train, when high speed operational conditions are considered. This system should ideally operate with relatively low contact forces and no contact loss should be observed, so that the power be constant.

A thermal analysis of this system could help maintenance operations revealing, for example, overheating of the pantograph strip and contact wire. In [1] the pantograph-overhead contact wire system is investigated by using an infrared camera. According to the results of finite element analysis and the temperature measurement of the tested pantograph pan, the effects of different heat sources caused by electric arc, contact resistance and friction were studied systematically on various pantograph pan materials in [10].

The effects of friction and electrical phenomena govern the wear rate in the sliding contact between pantograph collector strip and contact wire [3].

Heat transfer through interfaces formed by the mechanical contact of two non-conforming rough solids is an important phenomenon. Real surfaces have roughness and surface curvature/out-of-flatness simultaneously. Because of surface roughness, contact between two surfaces occurs only over microscopic contact spots [11].

In proposed paper, for thermal analyses of the system pantograph-contact line, we had made experimental determination of temperature.

II. Contact Line – Pantograph System

The proper balance between the dynamic characteristics of the pantograph and the contact line depends on the quality of current collectors and on the longevity of the contact wire and inserts. The pantograph must support them with sufficient force to remain in permanent contact with the wire, but not unduly raise (fig.1), which would lose contact after the points of attachment [9].

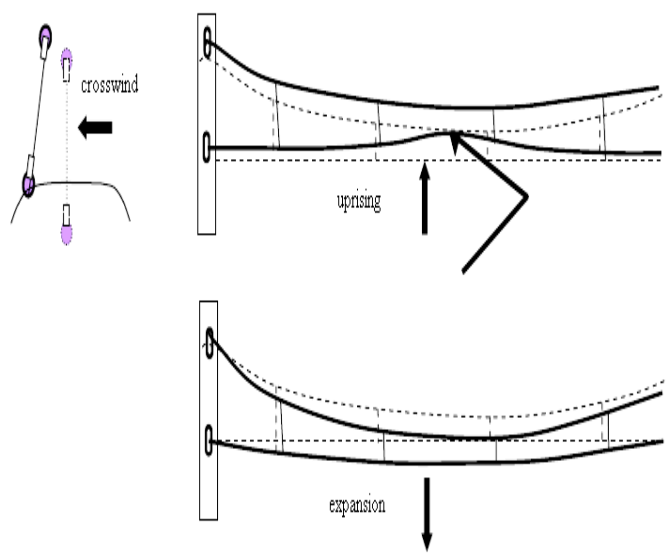

Fig.1. Factors influencing the dynamic behavior of the contact line

The circular section of the contact wire has two slots for the claws of catenary's suspensions (fig.2). According to the supply voltage and power requirements, the section ranges

F. A. Author is with Electrical Apparatus and Technologies, University of Craiova, Bd. Decebal, no. 107, 200440, Craiova, ROMANIA (e-mail: focoleanu@elth.ucv.ro).

S. B. Author, is with Electrical Apparatus and Technologies, University of Craiova, Bd. Decebal, no. 107, 200440, Craiova, ROMANIA (e-mail: ipopa@elth.ucv.ro).

T.C. Author is with Electromechanical, Industrial Information, Environment Engineering University of Craiova, Bd. Decebal, no. 107, 200440, Craiova, ROMANIA (e-mail: ghmanolea@gmail.com).

F. D. is with Electrical Apparatus and Technologies, University of Craiova, Bd. Decebal, no. 107, 200440, Craiova, ROMANIA (e-mail: adolan@elth.ucv.ro).

F.E. is with National Institute of Research INCDIE ICMET Craiova, Bd. Decebal, no. 107, 200440, Craiova, ROMANIA (e-mail: vlase_serghie@yahoo.com).

from 100 mm^2 to 150 mm^2. Produced by cold drawing, the section can be cylindrical or have a flat to increase the size of the sole contact with the friction of the device outlet. The cable must ensure good mechanical traction.

To decrease the electrical resistance of the line, the contact wire and cable are placed in parallel, at regular intervals using a copper shunt. The line is characterized by his "copper equivalence" expressed in mm². The different supply systems involve special design specifications (Table I), depending on the intensity carried [9].

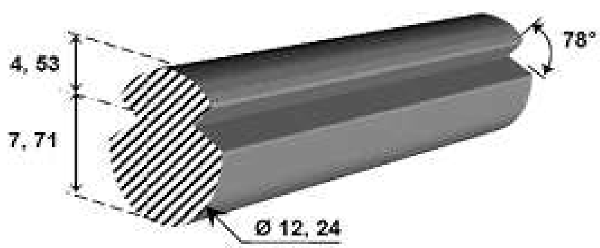

a) contact wire section

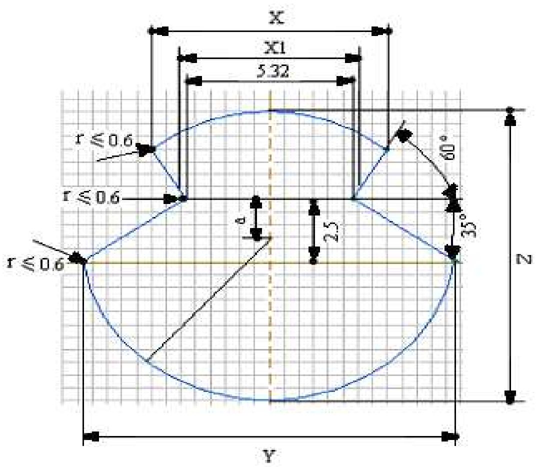

b) contact wire dimensions

Contact line wire	Section (mm²)	Erors (mm)	X (mm)	X1 (mm)	Y (mm)	Z (mm)	a (mm)	R (mm)
TF 100	100	±4	8.08 ±0.15	5.7 ±0.2	12.81 ±0.26	11.8 ±0.24	1.8	6.5

c) contact wire characteristics

Fig.2. Example of contact wire

Table I. Main features of some types of catenary

Contact line	Catenary	Contact line wire	Copper equivalent section	Weight m linear
tramway		copper disk 107 mm²	107 mm²	1,52 kg
1500 V compound	Principal : bronze - Sn 116 mm² Auxiliaire : 143 mm²	copper disk 2 × 150 mm²	480 mm²	5,309 kg
3000 V simple	copper 120 mm²	copper disk 2 × 100 mm²	320 mm²	2,85 kg
15 kV	steel-copper 92 mm²	copper 1 × 107 mm²	189 mm²	1,85 kg
25 kV	Al + steel 36 mm²	copper – Mg (Sn) 1 × 150 mm²	147 mm²	1,334 kg

In the plan, it is necessary that the laying of the contact line have a zig-zag from the center of the track, so that the contact point of the bow varies in time. A fixed point of contact would lead to the bow saw (fig.3).

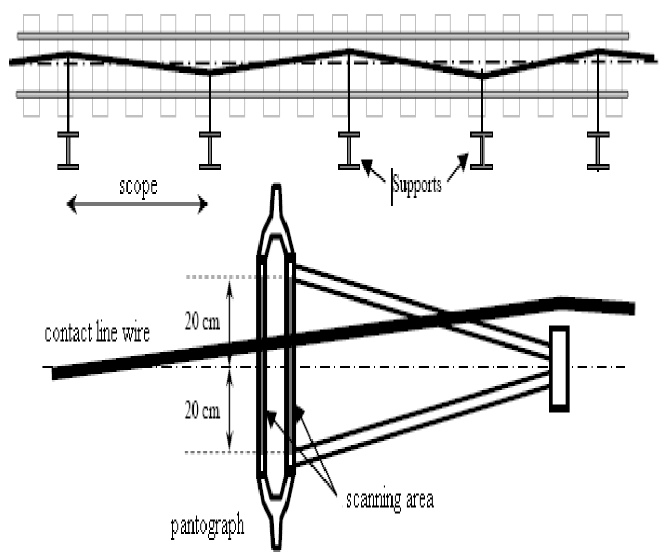

Fig.3 Desaxement periodic alignment

In curve, there should be a separation of materials compatible with the width of the bow, taking into account the possible cross movements.

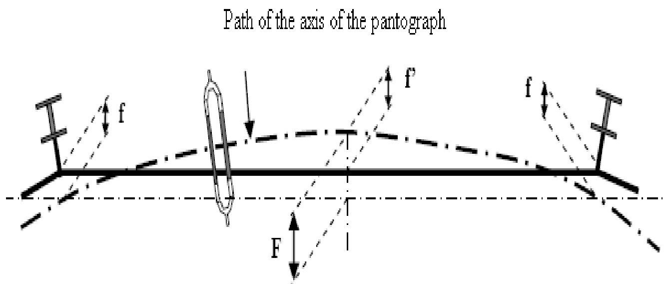

Fig.4 Desaxement curve
F: image of the curve in the range = a ² / 8R
f: desaxement the right support
f ': desaxement in the scope

The current collectors are now pantographs "light" that provide the power supply (fig.5).

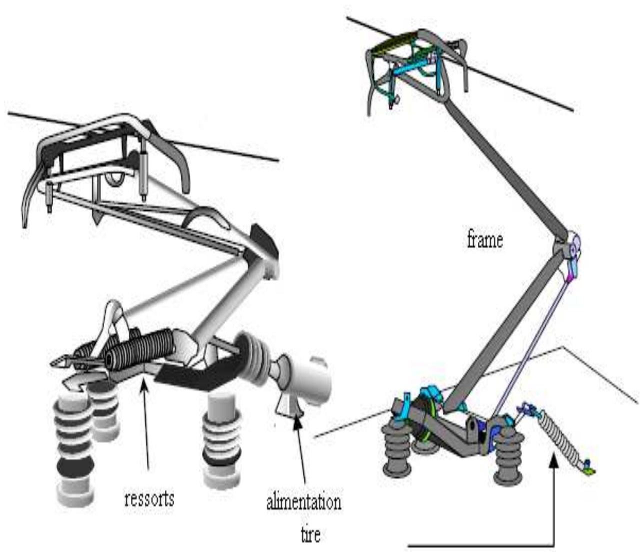

Fig.5 Examples of pantographs

III. Mathematical model

A *Mathematical model for contact wire*

The used mathematical model for determining the temperature in contact wire heating in A.C. current has two components, electromagnetic model and thermal model, both coupled through the source term (Joule specific loose).

$$S(\theta)=\rho(\theta)\cdot J^2(x,y) \tag{1}$$

Electromagnetic model

The electromagnetic model is governed by equation:

$$\frac{\partial}{\partial x}\left(\frac{1}{\mu}\cdot\frac{\partial A}{\partial x}\right)+\frac{\partial}{\partial y}\left(\frac{1}{\mu}\cdot\frac{\partial A}{\partial y}\right)-j\cdot\omega\cdot\sigma(\theta)\cdot A=-J \tag{2}$$

where :

- σ - is electric conductivity *;*
- μ is magnetic permeability*;*
- A is magnetic potential vector*;*
- j is imaginary unity *;*
- ω is pulsation ;
- J is current density.

Thermal model

The temperature distribution in the analysis domain is given by the thermal conduction equation in steady state:

$$\frac{\partial}{\partial \mathrm{x}}\left(\lambda\frac{\partial\theta}{\partial \mathrm{x}}\right)+\frac{\partial}{\partial \mathrm{y}}\left(\lambda\frac{\partial\theta}{\partial \mathrm{y}}\right)+S=0 \tag{3}$$

where :

- θ is temperature in celsius*;*
- λ is thermal conductivity*;*
- S is source term.

B *Mathematical model for contact pantograph strips – contact wire*

As well known, when two surfaces are in contact, the real contact area is much smaller than the nominal one.

The contact occurs in a finite number of asperities that are subjected to an elastic, plastic or combined elastic–plastic deformation depending on the normal pressure value, on the superficial roughness and on the material properties [5].

Existing theories/models for each part (macro and micro) are categorized based on the normal deformation mode of the bulk (substrate) and asperities into:

- elastic;
- plastic;
- elastoplastic.

Figure 6 illustrates the mechanical analysis overview for contact of spherical rough surfaces, which includes; a macro and a micro part [11].

Heat transfer through interfaces formed by the mechanical contact of two non-conforming rough solids is an important phenomenon.

Heat flow is constricted to pass through the macrocontact and then microcontacts (fig.7). This phenomenon is indirectly observed through a relatively high temperature drop across the interface[11].

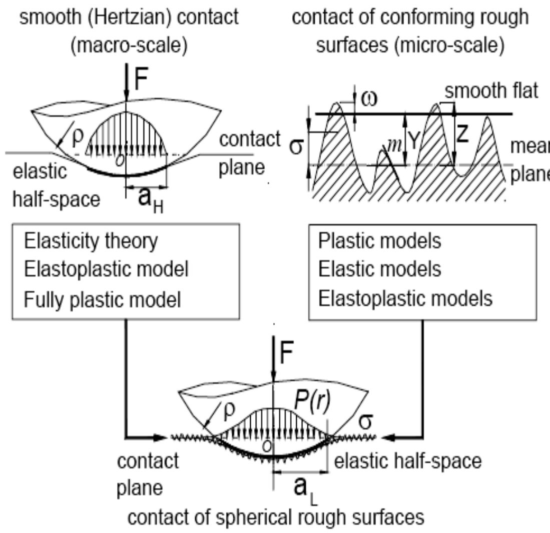

Fig.6 Mechanical problem overview for spherical rough surfaces

Thermal energy can be transferred between contacting bodies by three different modes:

- conduction at the microcontacts;
- conduction through the interstitial fluid in the gap between the contacting solids;
- thermal radiation across the gap.

The radiation heat transfer remains small, less than two percent of the conduction through the microcontacts, in the range of interest, Tc ≤ 100 ºC. Therefore it can be neglected for most engineering applications.

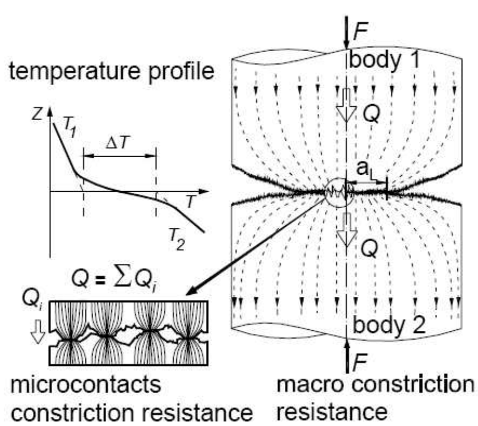

Fig.7 Non-conforming rough contact

Greenwood and Williamson [5] are the first authors that proposed a descriptive model for the contact between rough surfaces, which is still a benchmark for this research field. The Greenwood–Williamson (GW) model is based on the fact that the contact between two rough surfaces can be considered as an equivalent contact between a rough surface and a smooth surface (Fig.8). Each asperity is modeled with a spherical shape with uniform radius of curvature whose height above a reference plane has a normal (Gaussian) probability density function. The hypotheses of G-W model are:

- the asperity is spherical;
- the asperities are far apart and there is no interaction among them;
- during the contact, deformation only occurs for the asperities.

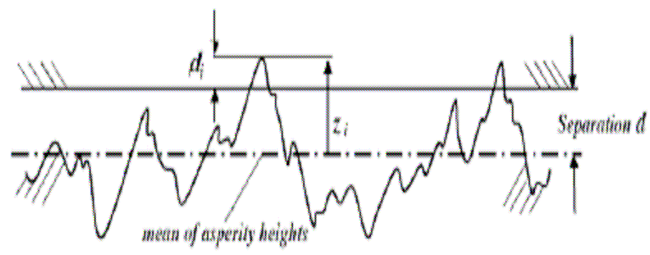

Fig.8 Contact between rough surfaces modeled as contact between a rough surface and a smooth surface

The real contact area can be calculated [3]:

$$A_r = \pi \cdot \beta_{GW} \cdot A_n \cdot (e^{-\lambda \cdot d^*} + e^{-\lambda \cdot (d^* + \delta_{cr})}) \tag{4}$$

where - β_{GW} is the roughness parameter;

- A_n is nominal contact area- λ is coefficient of exponential distribution;

- d^* is standard value of the mean separation d;

- δ_{cr} is standard value of the critical interference at the inception of plastic deformation.

β_{GW} , d^*, δ_{cr} are defined as:

$$\beta_{GW} = \eta \cdot r \cdot \sigma \tag{5}$$

$$d^* = \frac{d}{\sigma} \tag{6}$$

$$\delta_{cr} = \left(\frac{\pi \cdot K \cdot H}{2 \cdot E} \right)^2 \cdot r \tag{7}$$

where - η is surface density of asperities;

- r is radius of curvature of asperity;

- σ is standard deviation of asperities heights;

- d is mean separation;
- K is the ratio between the contact pressure that gives rise to a plastic deformation and the hardness of material H, considered equal to 0.6;
- E is elastic modulus.

Values for β_{GW}, η, r, σ, K and E are given in the Table II [5].

Table II The main values of statistical parameters, both for copper and for graphite strips

Parameter	Value for copper	Value for graphite
Coefficient of exponential distribution, c (Eq. (10))	0.115	0.06
Coefficient of exponential distribution, λ (Eq. (10))	0.178	0.102
Standard deviation of asperity heights, σ	7.349	11.383
Radius of curvature of asperity summits, r [µm]	30	70
Area density of asperities, η [1/µm^2]	400×10^{-6}	300×10^{-6}
Hardness of material, H [N/mm^2]	700	17
Equivalent elastic modulus, E' [N/mm^2]	72,500	4833
Nominal contact area, A_n [mm^2]	300	300
Initial arithmetical mean roughness of surface, R_a [µm]	1.1	2.9

The mean separation d is calculated using the probability density function $\phi(z)$:

$$\phi(z) = c \cdot e^{-\lambda \cdot z} \tag{8}$$

$$d = \int_0^{\infty} z \cdot \phi(z) dz \tag{9}$$

In [11] the author made a comparison of three models (Greenwood and Williamson model, Cooper, Mikic, and Yovanovich model and Tsukizoe and Hisakado plastic model) and he conclude that despite the different basic assumptions and input parameters in the GW elastic and Cooper, Mikic, Yovanovich and Tsukizoe, Hisakado plastic models, their behavior in terms of real contact area, size and number of microcontacts, and the relationship between the external force and real contact area are comparable in the applicable range of the separation.

IV. NUMERICAL DETERMINATIONS

A Analysis domain and boundary conditions

For stabilized temperature determination in the contact line wire in alternative current, has used a coupled problem AC magnetic – steady state heat transfer in Quick Field Professional (version 5.4).

The model of contact line wire is presented in figure 9.

The boundary condition for electromagnetic model is $A = 0$ on Γ_2 and for thermal model is of convection type (α, T_0) on Γ_1.

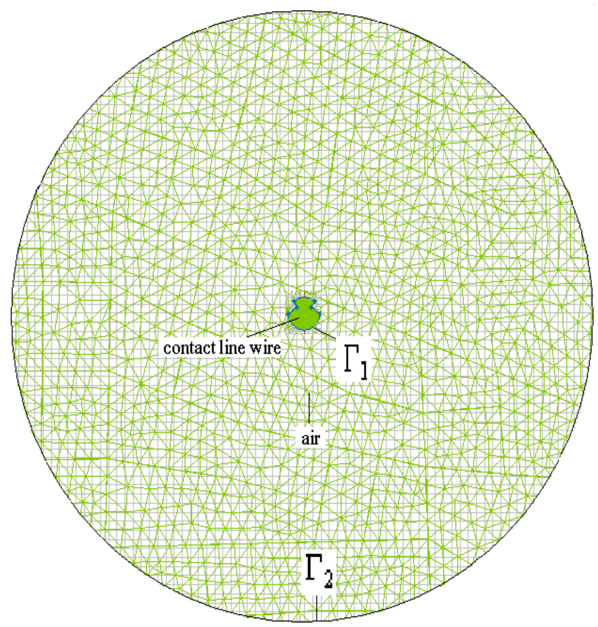

Fig. 9. Contact line wire model

B *Numerical results*

We have solved an electromagnetic and thermal field coupled problem for determination the stabilized temperature value for alternative current.

One determined the temperature values by neglecting the resistivity variation with temperature $\rho(\theta)$).

The current density distributions in contact line wire for 201 A, and 301 A , A.C are shown in figure 10 and figure 11.

In figure 12 and figure 13 are shown temperatures values for 201 A , 301 A, AC current.

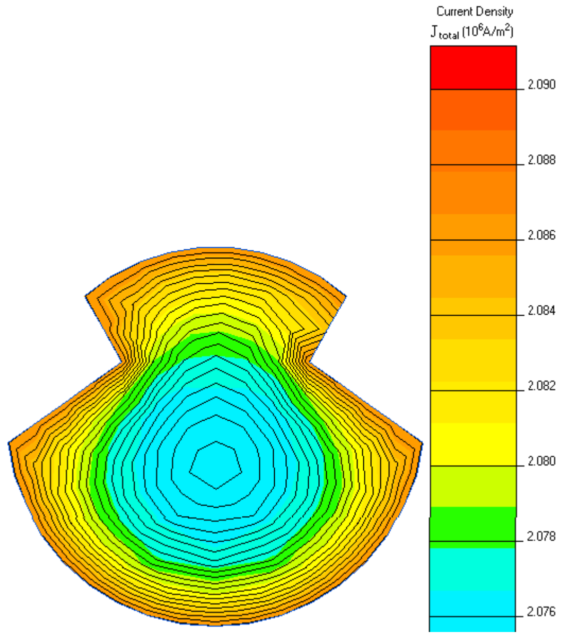

Fig. 10. The current density distributions – AC current, i=201A

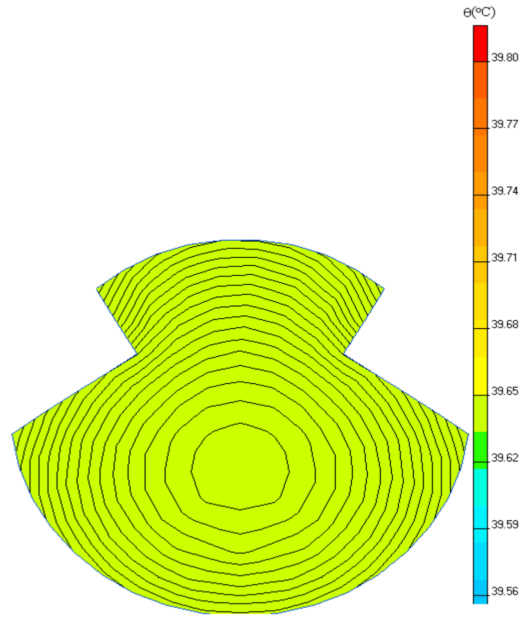

Fig. 12. Temperature in contact wire –AC current , i=201A, θ_0=22.7 °C

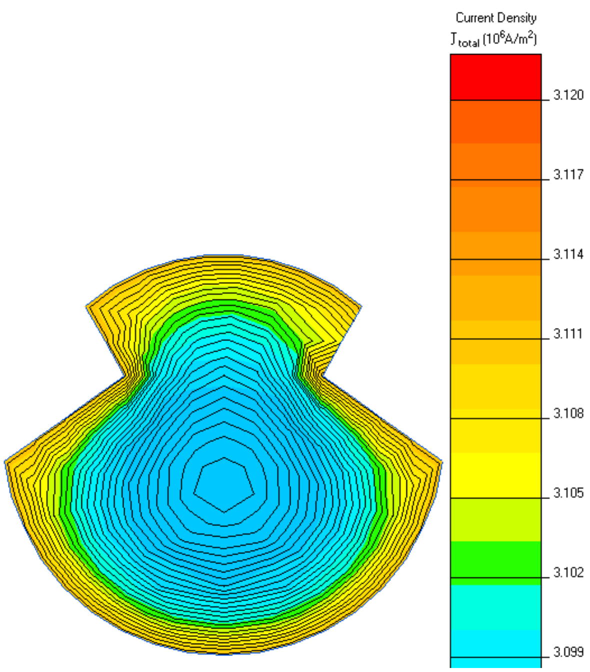

Fig. 11. The current density distributions – AC current, i=301A

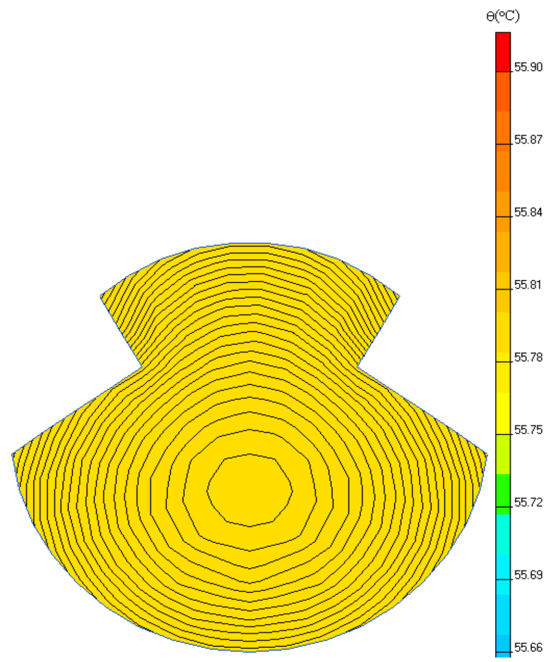

Fig. 13. Temperature in contact wire –AC current , i=301A, θ_0=23.5 °C

V. EXPERIMENTAL DETERMINATIONS

Experimentally we obtained the temperature in contact wire and in contact pantograph strips – contact line, A.C., for different values of the current. We performed a static determination, considering that the locomotive is not moving. The current absorbed by the locomotive is necessary for auxiliary services.

The considered pantograph is asymmetric EPC type and the contact line wire is TF 100 type, 100 mm^2 section, both used in Romanian Electric Railways.

The contact between two collector strips of pantograph and contact wire is made on a small surface as can be seen in figure 14, 15, 16.

The measured temperatures in contact wire for different current values, 201 A, 301 A and 403 A, AC are shown in figure 17, 18, 19, where $\Delta\theta = \theta_{max} - \theta_0$, ($\theta_0$ is ambient temperature in Celsius and θ_{max} is temperature in the wire).

The measured temperatures in contact pantograph strips – contact line, A.C, for different current values, 15 A, 20 A and 25 A, AC are shown in figure 20, 21, 22. The measurement were made for an ambient temperature of 20 ºC.

Thermal analyses is made by measuring temperatures in contact pantograph strips – contact line and with infrared thermovision camera.

Fig. 14 Contact zone

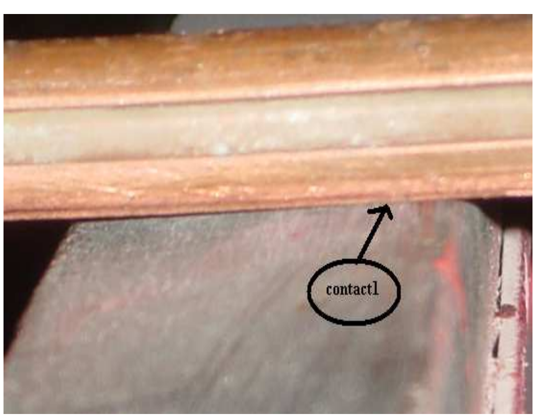

Fig.15 Contact zone 1

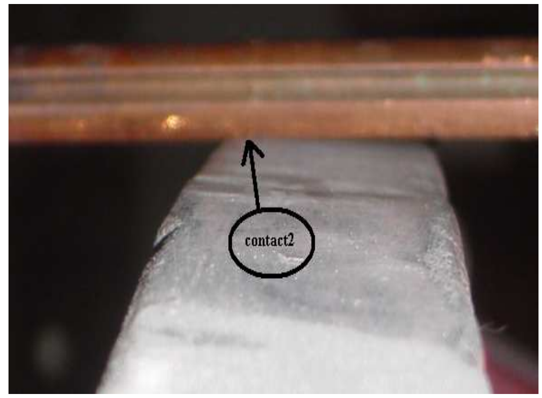

Fig.16 Contact zone 2

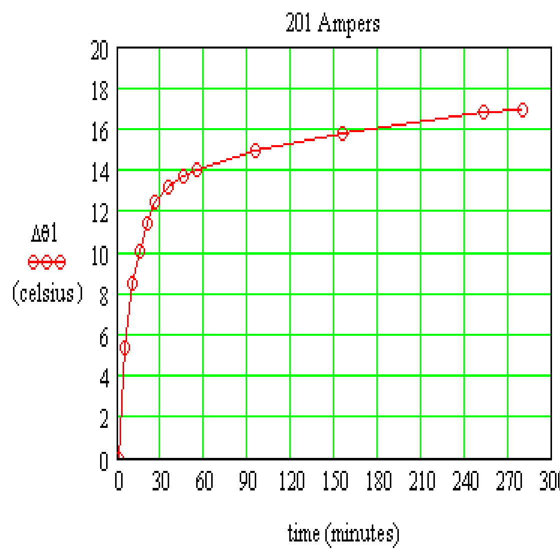

Fig.17 Contact wire temperature evolution for 201 ampers, A.C. current

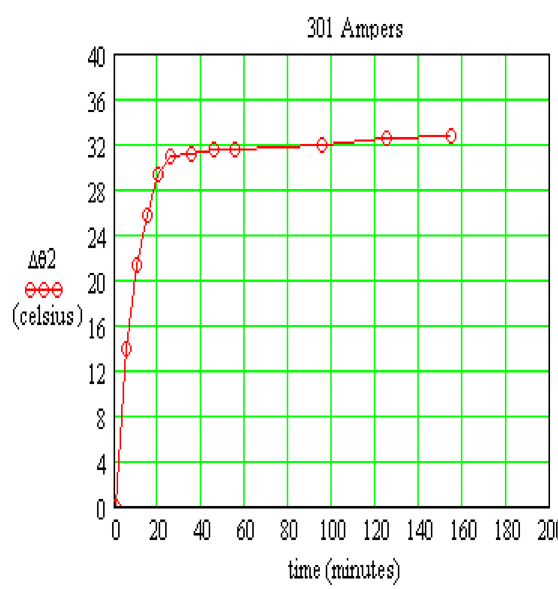

Fig.18 Contact wire temperature evolution for 301 ampers, A.C. current

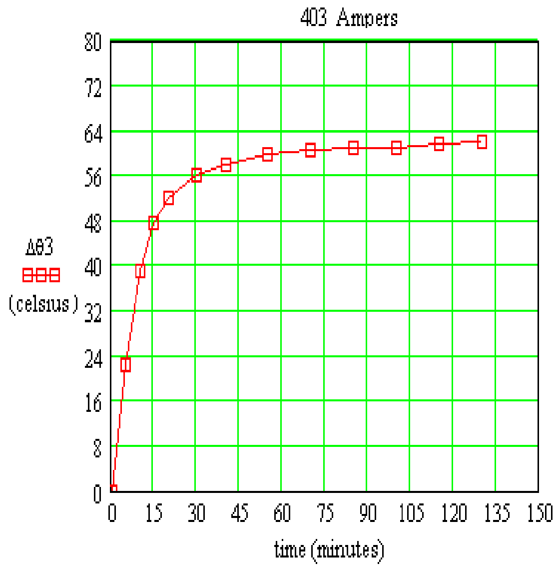

Fig.19 Contact wire temperature evolution for 403 ampers, A.C. current

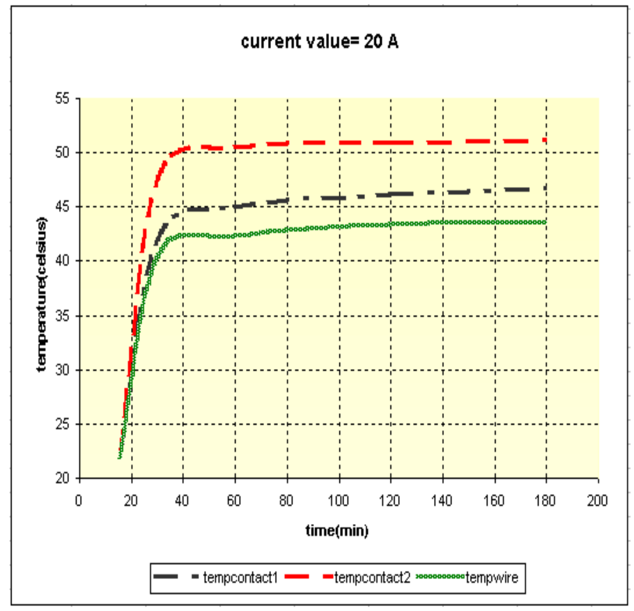

Fig. 21 Measured temperatures in contact for 20 A, AC current

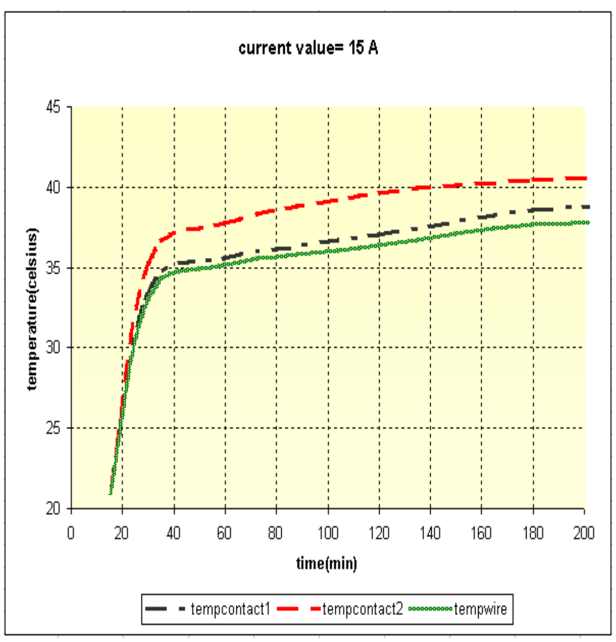

Fig. 20 Measured temperatures in contact for 15 A, AC current

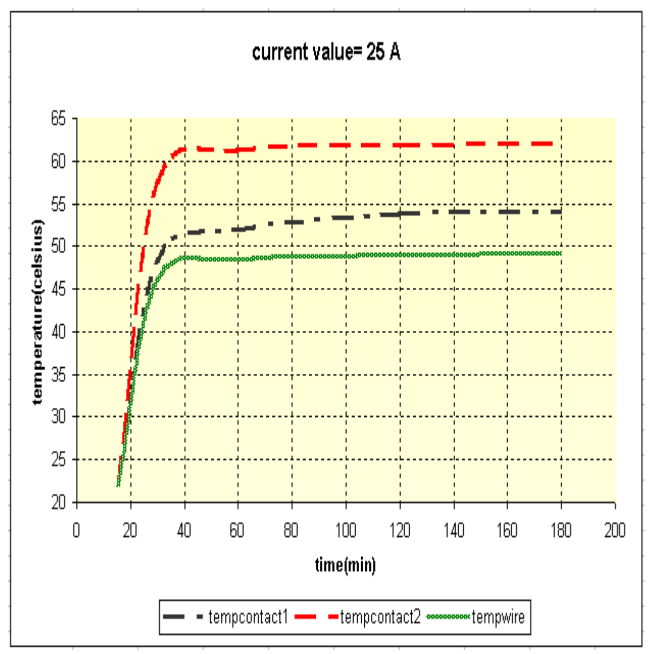

Fig. 22 Measured temperatures in contact for 25 A, AC current

In figure 23 and figure 24 are shown the thermal spectrums of system with infrared thermovision camera. It can be seen from this figure the hot contact spots.

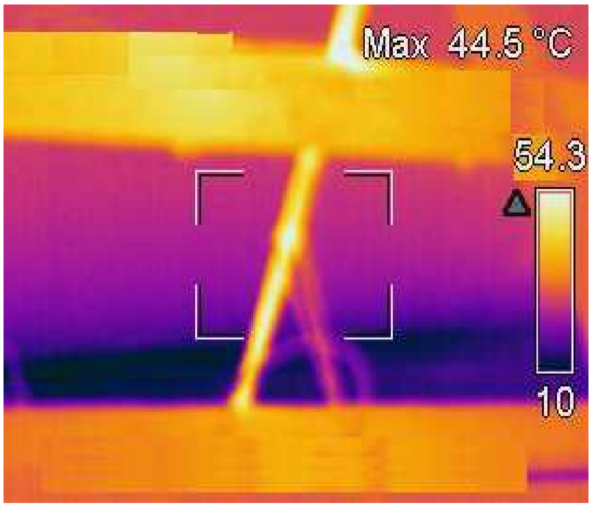

Fig. 23 Infrared camera's view 1

Fig. 24 Infrared camera's view 2

VI. Conclusion

The experimental results show an increase of temperature value in both contacts for a small current value at an ambient temperature of 20 ºC. The influence on temperature of contact area is evident. The temperature in contact 2 is bigger than in contact 1 because of his smaller contact area.

In the wire between the two contact areas the temperature is nearly to the value in contact 1.

In future, an analytical and numerical model of contact pantograph-contact line for evaluating the temperature values will be developed. Numerical model must take into account the resisivity variation with temperature.

The obtained model will be validated by these experimental results.

References

[1] Landi A., Menconi L., Sani L., *Hough transform and thermo-vision for monitoring pantograph-catenary system*, Proceedings of the Institution of Mechanical Engineers, Part F: Journal of Rail and Rapid Transit, Vol. 220, no. 4, pp. 435-447, 2006.

[2] He D.H., Manory R., Grady N., *Wear of railway contact wires against current collector materials*, Wear 215, pp. 146–155, 1998.

[3] Bucca G, Collina A., A procedure for the wear prediction of collector strip and contact wire in pantograph–catenary system, Wear 266, pp. 46–59, 2009.

[4] Jamari J., Schipper D.J., *Experimental Investigation of Fully Plastic Contact of a Sphere Against a Hard Flat*, Transactions of the ASME, Vol. 128, pp. 230-235, April 2006.

[5] Greenwood J .A., Williamson J. B. P., *Contact of nominally flat surfaces*, Proceedings of the Royal Society Series A295, pp. 300–319, 1966.

[6] Balestrino, A., Bruno, O., Landi, A., Masini, P., Mingozzi, E., Papi, M., and Sani, L. *Infrared camera for monitoring pantograph-catenary interactions*, Proceedings of World Conference of Railway Research, Edinburgh, UK, pp. 1-7, 2003.

[7] Ocoleanu C.F., Popa I., Manolea Ghe., *Study of the Skin Effect Influence on Electric Railway System Supply Line Heating*, Environmental problems and development, Proceeding of the 1st WSEAS International Conference on Urban Rehabilitation And Sustainability - URES 2008, pp. 142-146, Bucharest, Romania, November 7-9, 2008.

[8] Rauter F.G, Pombo J., Ambrosio J., Chalansonnet J., Bobillot Adrien, *Contact model for the pantograph-catenary interaction*, Journal of System Design and Dynamics, Vol. 1, no. 3, 2007.

[9] Cividjian G.A., Pascu Ileana, Bunescu A., Matei D.M., Dolan A., *Experimental study of the resistance of flat Cu-W contacts*, XII-th International Symposium on Electrical Apparatus and Technologies - SIELA 2001, Vol. I, pp. 58-65, Plovdiv, Bulgaria, May 31 - June 1st, 2001.

[10] Dai L., Lin J., Liu Y., Ding X., *Calculation and study on strip cubage temperature of pantograph pan in sliding electric contact abrasion*, Journal of the China Railway Society, Vol. 24, no. 5, pp. 56-61, Sept.-Oct, 2002.

[11] J. A. Greenwood, K. L. Johnson, and M. Matsubara, "A surface roughness parameter in hertz contact," Wear, vol. 100, pp. 47—57, 1984.

[12] Majid Bahrami, *Modeling of Thermal Joint Resistance for Sphere-Flat Contacts in a Vacuum,* Thesis, Waterloo, Ontario, Canada, 2004.

[13] F. H. Milanez, J. R. Culham, and M. M. Yovanovich,"Comparisons between plastic contact Hardness models and experiments," AIAA Paper No.2003-0160,41th AIAA Aerospace Meeting and Exhibit, Jan. 6-9, Reno, Nevada., 2003.

[14] Y. Zhao, D. M. Maietta, and L. Chang, "An asperity model incorporating the transition from elastic deformation to fully plastic flow," Journal of Tribology, Trans. of ASME, vol.122, pp. 86—93, 2000.

[15] Rauter Frederico Grases, Pombo Joao, Ambrosio Jorge, Chalansonnet Jerome, Bobillot Adrien, Pereira Manuel Seabra, *Contact model for the pantograph-catenary interaction*, Journal of system, design and dynamics, vol.1, no.3, 2007.

[16] Schaub M., Simeon B., "Pantograph-Catenary Dynamics: An Analysis of Models and Simulation Techniques", in *Mathematical and Computer Modeling of Dynamical Systems*, vol. 7, n. 2, pp. 225-238, 2001.

[17] Jesús Benet, Angelines Alberto, Enrique Arias, Tomás Rojo, *A Mathematical Model of the Pantograph-Catenary Dynamic Interaction with Several Contact Wires*, IAENG International Journal of Applied Mathematics, 37:2, IJAM_37_2_10.

[18] Drugge L., Larsson T., Stensson A., "Modelling and Simulation of Catenary-Pantograph Interaction", in *Vehicle System Dynamics*, vol. 33 (supplement), pp. 490-501, 1999.

[19] Lesser M., Karlsson L., Drugge L., "An Interactive Model of a Pantograph-Catenary System", in *Vehicle System Dynamics*, vol. 25 (supplement), pp. 397-412, 1996.

[20] J. A. Greenwood and J. J. Wu, "Surface roughness and contact: An apology, " Meccanica, Kluwer Academic Publishers, vol. 36, pp. 617—630, 2001.

[21] Popa I., Cauțil I., Floricău D., Ocoleanu F., Modeling of high currents dismountable contacts, *8th International Workshop Computational of Electrical Engineering,* September 14 – 16, Wilkasy, Poland, Book of Abstracts, pp. 44-47, 2007.

[22] Popa I., Cauțil I., Influence of Skin Effect on the Temperature Distribution in a Cylindrical Current Leads, *International Symposium on Electrical Apparatus and Technologies (SIELA 2005),* Plovdiv 2 – 3 June, Bulgaria, pp. 119 – 124, 2005.